frontiers | Frontiers in Mechanical Engineering

TYPE Original Research
PUBLISHED 22 February 2023
DOI 10.3389/fmech.2023.1120985

OPEN ACCESS

EDITED BY
Giancarlo Sorrentino,
Istituto di Scienze e Tecnologie per l'Energia e la Mobilità Sostenibili (STEMS)—CNR, Italy

REVIEWED BY
Lorenzo Giuntini,
University of Pisa, Italy
Lorenzo Frascino,
National Research Council (CNR), Italy
Alessio Picchi,
University of Florence, Italy

*CORRESPONDENCE
Ashraf Kotb,
Ashraf_Ibrahim@eng.asu.edu.eg

SPECIALTY SECTION
This article was submitted to Heat Transfer Mechanisms and Applications, a section of the journal Frontiers in Mechanical Engineering

RECEIVED 10 December 2022
ACCEPTED 30 January 2023
PUBLISHED 22 February 2023

CITATION
Kotb A, Askar H and Saad H (2023), On the impingement of heat transfer using swirled air jets.
Front. Mech. Eng 9:1120985.
doi: 10.3389/fmech.2023.1120985

On the impingement of heat transfer using swirled air jets

Ashraf Kotb[1]*, Hamada Askar[2] and Hany Saad[1]

[1]Department of Mechanical Power Engineering, Facuty of Engineering, Ain Shams University, Cairo, Egypt, [2]Department of Math and Physics, Facuty of Engineering, Ain Shams University, Cairo, Egypt

Experimental analyses were conducted under identical experimental conditions on the heat transfer between a constant heat flux flat plate and a round air jet for both conventional and swirled jets. Vane-type swirl generators inserted at the nozzle exit were used to produce a swirl. The experimental measurements were performed at a fixed Reynolds number value (Re = 23,000) calculated on the jet tube's inside diameter. A comparison between conventional air jets and swirl jets with swirl numbers of S = 0, 0.19, 0.42, and 0.72 was presented for the different nozzle-to-plate spacings Z/D = 2, 6, and 10. The results show that heat transfer to the plate decreases when the nozzle-to-plate distance increases. In addition, increasing the swirl number S increases heat transfer uniformity but decreases global heat transfer. At the low plate-to-jet distance Z/D = 2, the point of maximum heat transfer is shifted to a radial position depending on the swirl number. Also, for both Z/D = 6 and 10, the stagnation point and stagnation region heat-transfer enhances only for swirl numbers 0 and 0.19.

KEYWORDS

jet impingement, impingement heat transfer, swirling air jet, combustion, energy

1 Introduction

Jet impingement heating and cooling are used as techniques for achieving a high local and average heat transfer coefficient resulting in higher heat transfer rates (Martin, 1977). It has therefore been employed in many engineering applications, such as cooling tempering glass, turbine blades, hot steel plates, and turbine electronic components, and drying film and paper (Oztekin et al., 2012). Jet impingement is not limited to cooling applications but is also applied to the heating and mass transfer processes (Ahmed et al., 2016; Ahmed et al., 2017).

The common feature in impingement heat transfer is to enhance heat transfer in the stagnation region in addition to the wall rapid decay of heat transfer to the jet region. This is due to the boundary layer buildup on the target plate surface. The characteristics of jet flow are highly complex and, consequently, heat transfer from a surface to jet flow is highly variable (Nuntadusit et al., 2012). Much experimental work has been conducted to discover the parameters that influence fluid flow and heat transfer. Jet impingement is affected by the flow condition at the nozzle exit, flow Reynolds number (Re), type of jet (conventional/swirled), jet-to-plate spacing (Z/d), (normal/inclined) jet, round or rectangular, degree of swirl, shape of swirl, the nozzle shape (circular, slit, triangle, etc.), degree of jet inclination, and surface type (flat/curved) (Hattori and Nagano, 2004; Alekseenko et al., 2007; Tesar, 2009; Nuntadusit et al., 2012).

Baydar (1999) studied impinging air-jet fluid flow characteristics using single and double jets for both laminar and turbulent conditions. He concluded that the sub-atmospheric region took place up to a nozzle-to-plate distance of two nozzle diameters for Reynolds numbers higher than 2,700. Duda et al. (2008) investigated the behavior of a round jet with a

straight tube, in addition to measuring the turbulence intensity and velocity at the jet outlet by using a smoke wire visualization technique.

Yang et al. (1999) studied cooling heat-transfer jet impingement characteristics on a semi-circular concave surface for the effects of both the curvature of the plate and the nozzle geometry on the average value of the heat transfer coefficient. They found that the average heat transfer rates for impingement are higher for the concave surface than for the flat plate. Garimella and Nenaydykh (1996) and Colucci and Viskanta (1996) investigated jet impingement cooling for a flat plate to determine the effect of different geometries of the impingement nozzle on the local convective heat transfer rate. They found that the local heat transfer coefficients are affected by the Reynolds number and the nozzle-to-plate spacing more for confined than unconfined jets. The flow characteristics for the turbulent jet impinging on a flat plate review report are presented by Gauntner et al. (1970).

Öztekin et al. (2013) mathematically and experimentally investigated the characteristics of heat transfer on concave plates for a turbulent-impinged air slot jet. They found that, by increasing both Reynolds number and nozzle-to-plate distance, the average Nusselt numbers decreased. They stated the effect of the curvature radius on the characteristics of heat transfer.

Swirl flow can be generated by directing the axial flow through vanes inserted at the nozzle exit. Investigations have used many different designs for swirl generators for jets. The degree of swirl affects the entrainment of ambient air, the degree of jet expansion, and jet decay. Many researchers have studied swirl effects on flow and heat transfer characteristics. Ward and Mahmood (1982) designed the first swirling impinging jet by using naphthalene sublimation to investigate the effect of heat and mass transfer characteristics on a flat target surface.

Huang and El-Genk (1997) generated a swirling flow with four narrow channels of a cylindrical plug to provide swirling flow to single and multiple air-impinging jets. They concluded that radial heat transfer distribution is uniform at a high swirl degree and large distance between the plate surface and the jet for single jet impingement with a swirl.

Lee et al. (2002) investigated the effect of eight narrow channels of a swirling jet on local and average heat transfer distribution. For a small distance between the jet and the plate surface ($Z/D = 2$), the average swirling jet flow Nusselt number is larger for all swirl degrees used than those without swirl, but, for $Z/D > 10$, the effect of swirling jet flows was less significant.

Wen and Jang (2003) designed swirling strips for insertion in the jet nozzle and showed that crossed swirling strips have better heat transfer performance than standard jets. Owsenek et al. (1997) conducted a numerical investigation of impinging radial and axial laminar jets with superimposed swirls on a flat plate using the solution of Navier–Stokes and energy equations. They concluded that heat transfer from the superposition of swirl on axial jets is substantially reduced but observed a significant enhancement in heat transfer with a radial jet. Ianiro and Carlomagno (Cardone and Carlomagno, 2010) conducted an experimental investigation using helical inserts, based on the design of crossed swirling strips developed through quick prototyping. They concluded that mean heat transfer decreases with increased nozzle-to-plate distance. Increased distance leads to an increase in the uniformity of heat transfer. The increased swirl number produces increased uniformity but decreased total heat transfer.

Burak Markal (2018) conducted an experimental study of swirling coaxial confined impinging turbulent air jet-flow characteristics using different nozzle-to-plate distances and dimensionless flow rates. He analyzed the pressure distribution and heat transfer characteristics on the impingement plate. The results showed that, with an increase in the flow rate ratio, the average Nusselt number increases and enhances the uniformity of the heat transfer through the impingement surface.

Debnath et al. (2020) conducted a numerical examination of circular multiple jets using two different array types and of the swirl effect on impingement jets using a flat surface with a jet-to-plate distance equal to $H = 2D$, where D is the nozzle diameter. They found that staggered arrangements improved heat transfer characteristics. They also concluded that the recirculation strength of a swirling jet is larger than that of a non-swirling jet.

Ikhlaq et al. (2019) compared both swirling and non-swirling transient flow development. Liang Xu et al. (2021) proposed a new swirling impingement cooling jet with four inner spiral grooves in internal threads. They experimentally investigated the heat at different swirl angles from 0° to 45° and different Re and jet-to-plate distances. They concluded that the scattering region of the jet airflow from the nozzle is large at a large swirl angle. Ahmed-Zahir et al. (2016) studied the effect of tangential impinging swirl jet on heat transfer characteristics. They found that using low and medium swirl angles at a certain Reynolds number improved the value of Nu compared with a conventional jet.

Tao Yang et al. (2023) studied the characteristics of the heat transfer of four different nozzle types with different swirl numbers. They compared experimental with numerical work at different Re from 6,000 to 12,000 and studied the effect of changing swirl angle θ and Re on the Nu of all nozzles. They found that increasing the swirl angle enhances heat transfer characteristics.

Prashant Singh et al. (2023) and Gerardo Paolillo et al. (2022) studied the effect of the jet-to-plate distance effect on heat transfer characteristics.

The objective of this research is to investigate the characteristics of the impingement cooling of a flat plate with constant heat flux with and without an air-jet swirl generator and different jet-to-plate distances in order to enhance heat transfer characteristics. The nozzles are fed from a long straight tube. Such a feeding system could be used for cooling electronic devices, plate glass tempering, and for drying paper. The flow entrainment, jet spreading rate, and turbulence characteristics at the exit swirl nozzle would increase before impinging on the target plate. This study used a new vane-type swirl generator with six external spiral narrow channels. Two-dimensional measurements of the convective heat transfer between a target flat plate and impinging swirling air jet were made for different distances (nozzle to plate) and different swirl angles. In order to study the swirl number effect on the heat transfer distributions near the stagnation point region, the results obtained were used to compare the swirled jets and conventional jets at the same experimental conditions. The results can be used to provide additional reference for developing a new swirling impingement nozzle for cooling for high-performance heat transfer.

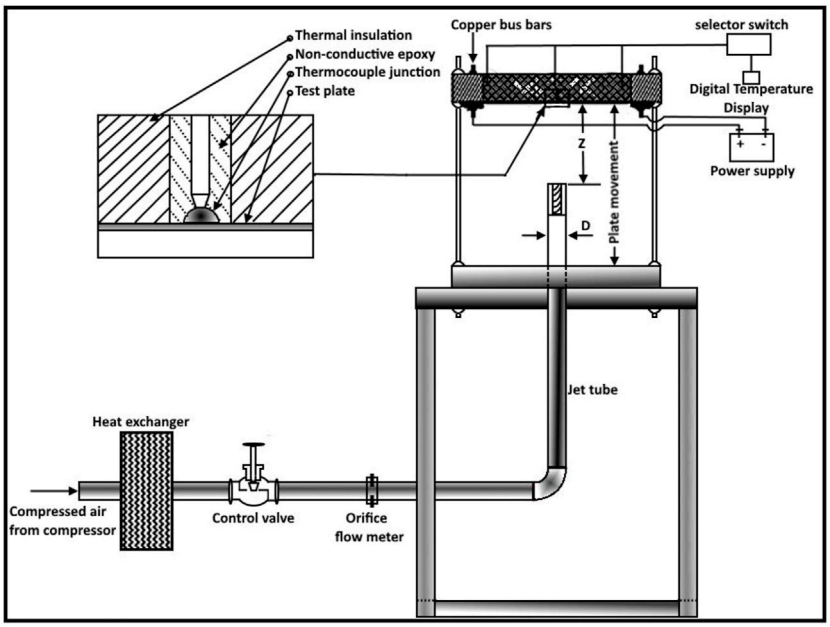

FIGURE 1
Experiment's schematic diagram.

2 Experimental apparatus and procedures

The experimental test rig is shown in Figure 1. The test rig was used to study the heat transfer characteristics of the impingement jets of a single nozzle without swirl or with different swirl angles in addition to different jet-to-plate spacings by adjusting the height of the plate.

The rig consisted of a stainless-steel plate, (304) 220 mm wide, 300 mm long, and 0.4 mm thick. Two copper bus bars were connected to the plate's far opposite ends. A DC current was supplied to the copper bus bars through a variable voltage transformer. Voltage and current were kept constant during all experiments to fix the input energy to the plate. The other two ends—thin compared to the plate surface area—were insulated. Distributed in both X and Y directions were 61 calibrated K-type thermocouples planted in the rear of the test plate to measure plate temperature distribution. The thermocouples form a two-dimensional mesh with a uniform mesh spacing of 5 mm. A data acquisition system recorded the measured temperature type NI9214, compensating for atmospheric temperature. To reduce the heat transfer losses from the plate, the back side of the test plate was thermally insulated with low thermal conductivity material using a 10-mm-thick fiber plastic plate made from carbon, placed in a box made of wood and padded with fiberglass.

The bottom plate surface was exposed to the impinging jet through an air-jet nozzle located below the plate (Figure 1). The plate holder was equipped with a mechanism to change the plate level so that the jet-to-plate distance z could be changed. The air jet was perpendicular to the plate and its centerline lay on the geometric center of the plate.

FIGURE 2
Swirl generators used in the experiment.

The test rig consisted of an air compressor equipped with an air filter. A dehumidification system was used.

The insulation of the plate ends and its top surface uniformly heated it by constant volumetric heat generation by an electric current flowing through the plate. This arrangement simulated the heating of the flat plate by a uniform heat flux. The perpendicular and central arrangement of the jet impinging on the plate caused the airflow pattern along the plate surface, as well as the plate temperature, to be symmetrical to the intersection of the nozzle axis and the plate surface.

Thermocouple terminals were attached to two selector switches. A digital temperature display with ±1% accuracy displayed the output of the thermocouples in degrees Celsius, in addition to the data acquisition system. Atmospheric air supplied by a compressor went through a pressure regulating

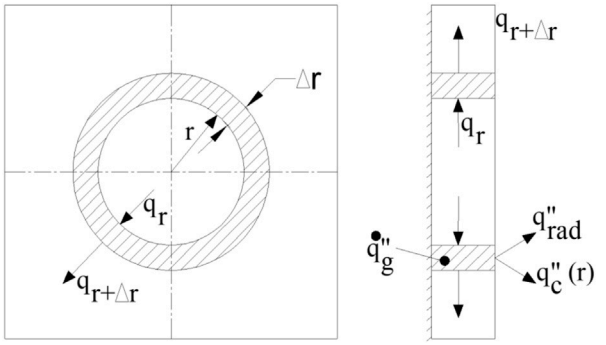

FIGURE 3
Differential control volume for heat balance analysis in the stainless-steel test plate.

valve to a heat exchanger that kept the jet temperature Ti within ±0.2°C of ambient room temperature. This air passed through a control valve to adjust the required airflow rate, then entered the calibrated orifice flowmeter, and, finally, the nozzle pipe.

Figure 2 shows the vane-type swirl generators used in the experiments. The swirl generators were made of copper; the length of each was L = 40 mm with an outer radius of R = 7.5 mm. Six vanes were used, each with a thickness of t = 2 mm.

The swirl number S was evaluated using Eq. 1 given by Lee et al. (2002):

$$S = \frac{2}{3}\left[\left(1-\left(\frac{r_1}{R}\right)^3\right)\Big/\left(1-\left(\frac{r_1}{R}\right)^2\right)\right]\tan\theta, \tag{1}$$

where θ is the angle between the vane axis and swirl vane and r and R are the inner and outer radii of the swirl generators, respectively.

For these swirl generators with angles of (0°, 15°, 30° and 45°), the corresponding swirl numbers according to Eq. 1 will be (0, 0.19, 0.42, and 0.72).

The orifice plate flowmeter, voltmeter, and current ammeter tolerances were 2.5%, 0.2%, and 0.2%, respectively. Accordingly, the maximum uncertainty in both Re and Nu was evaluated as 2.8% and 2.2%, respectively. The uncertainty formulas used to estimate the percentage error for Re and Nu are found in Xu et al. (2021).

3 Data analysis

3.1 Flow parameters

The jet's Reynolds number was calculated from the following equation:

$$Re = \frac{m^{\circ}D}{A_j\mu}, \tag{2}$$

where m° is the measured mass flow rate by the orifice flowmeter, D is the diameter of the jet tube, A_j is the cross-sectional area of the jet tube, and μ is the viscosity of air at the jet exit temperature.

3.2 Heat generation and transfer

The thickness of the test plate was small (δ = 0.4 mm), and the volume rate of heat transfer generation was uniform and constant as before. Thus, the rate of heat generation per unit volume of the plate q''' is given by

$$q''' = \frac{Volt \times Amp}{V}, \tag{3}$$

where *Volt* and *Amp* are the value of the voltage and the amperage of the power input across the bus bars, respectively, and V is the volume of the used plate.

For the steady-state rate, the energy equation for the circular element shown in Figure 3 takes the form:

$$\boldsymbol{q''_r - q''_{r+dr} - q''_k(r) + q''_g - q''_{rad} - q''_c = 0}, \tag{4}$$

where the net rate or radial conduction rate q''_k (r), represents the value of the terms ($q''_r - q''_{r+dr}$) in Eq. 4, is given by Greco et al. (2018):

$$\boldsymbol{q''_r = -k_p\frac{\partial T}{\partial r}, q''_k(r) = q''_r - q''_{r+dr} = \frac{\partial}{r}\frac{\partial}{\partial r}(k_p)(r\,\partial T/\partial r)}, \tag{5}$$

$$\boldsymbol{q''_{rad} = \varepsilon\sigma\left(T^4_w(r) - T^4_{sur}\right)}, \tag{6}$$

where $q''_c(r)$ is the local rate of convective heat transfer from the plate to the air flowing radially over the plate surface, q''_g is the rate of heat generation in the element equal to ($2\pi q'''\delta$), and q''_C is conduction heat loss through thermal insulation. The radial heat conduction term q''_r is induced by the temperature gradient in the radial direction r along the jet-impinged plate surface; it can be neglected for the thin plate as it is small compared to the heat generation term. q''_{rad} is the radiation heat loss from the plate surface. k_p is the thermal conductivity of the test plate. The local rate of convective heat transfer $q''_c(r)$ can be expressed as

$$\boldsymbol{q''_c(r) = q''_{rad} - q''_k(r) + q''_g}. \tag{7}$$

The radial conduction term q''_k (r) can be neglected (calculated from the measured values of the local plate temperatures) for the thin plate. Losses q''_c (r) through the insulation by conduction from the plate insulated surface by conduction through the insulation, and there from the insulation surface by natural convention, can be neglected due to the thermal insulation's low thermal conductivity.

$$\boldsymbol{q''_c(r) = q''_g - q''_{rad}}. \tag{8}$$

The local convective heat transfer coefficient for convective heat exchange between the impinging jet and the plate is calculated using the following equation as expressed by Yang et al. (2023):

$$\boldsymbol{h(r) = q''_c(r)/\left(T_w(r) - T_j\right)}. \tag{9}$$

The corresponding local Nusselt number is obtained as

$$\boldsymbol{Nu(r) = h(r)D/K_a}. \tag{10}$$

In Eq. 9, $T_w(r)$ is the local surface temperature, T_j is the jet exit temperature, D is the jet tube diameter, and k_a is the thermal conductivity of air evaluated at the jet exit temperature of air. Note that the heat transfer coefficient and the local Nusselt number obtained by this procedure are valid for impingement cooling as well as for impingement heating because their values

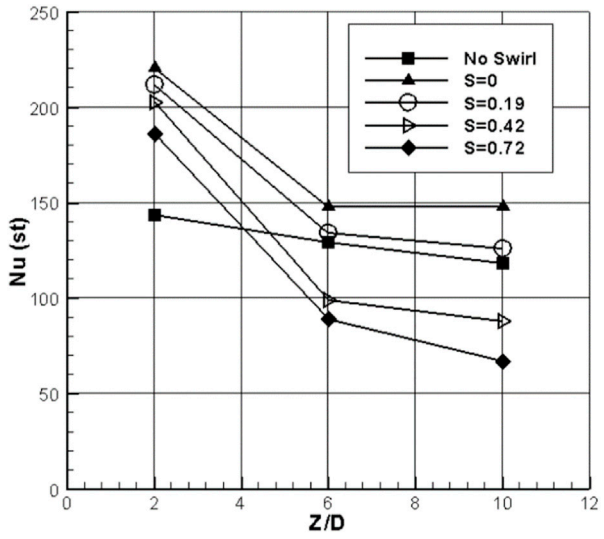

FIGURE 4
Stagnation point Nusselt number with Z/D at different swirl numbers.

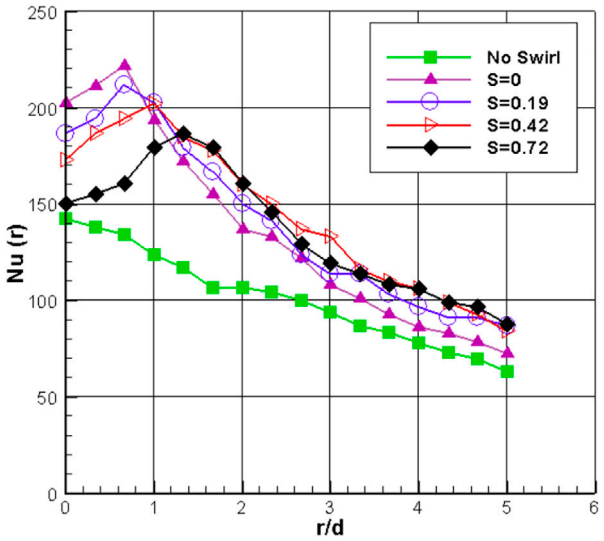

FIGURE 5
Local Nusselt number distribution with r/d at different swirl numbers for Z/D = 2.

are dependent on the airflow mode along the plate, with the Prandtl number varying with the air temperature.

3.3 Heat loss test

The input power (P_i) to the target plate used a DC current supply to the copper bus bars through a variable voltage transformer. This power was used to heat the plate. The system heat loss includes both the heat loss by radiation from the plate to the environment (H_{rad}) and by conduction through the insulation surface layer on the plate (H_{con}). By using these definitions, the heat flux (q") on the target plate surface can be defined thus:

$$q'' = (P_i - H_{rad} - H_{con})/A_{plate}.$$

Both the heat loss by radiation and the heat loss by conduction were experimentally calculated as less than 6% of the total power. The range of the heat loss for both conduction and radiation was 2.1–5.96 W and 1.95–5.8 W, respectively.

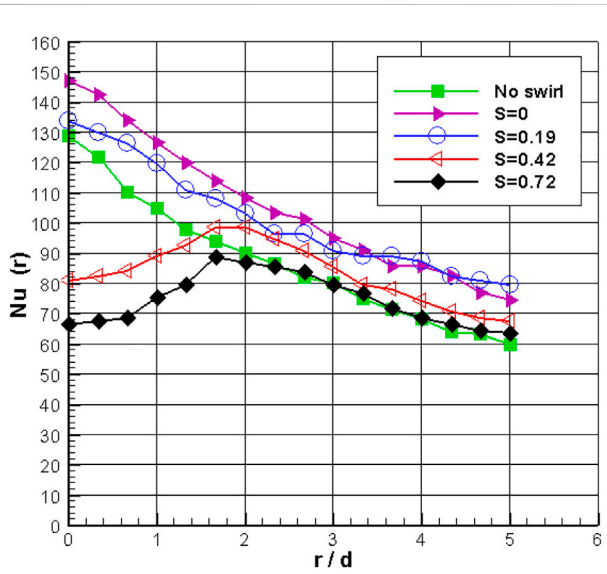

FIGURE 6
Local Nusselt number distribution with r/d at different swirl numbers for Z/D = 6.

4 Results and discussion

Figure 4 shows the variation stagnation point Nusselt number with different Z/D equal to 2, 6, and 10 at different swirl numbers and a jet Reynolds number equal to Re = 23,000. It is observed that the stagnation points' Nusselt number (Nu_{st}) has a strong dependence on the swirl number and jet-to-plate spacing (Z/D). Also, from this figure, it is evident that (Nu_{st}) at the same Reynolds number Re = 23,000 with S = 0 is higher than the jet with no swirl generator or S equal to 0.19, 0.42, and 0.72 at all Z/D spacing. At Z/D equal to both 6 and 10, the lower value of (Nu_{st}) at S = 0.72 while at Z/D = 2 is the lower value at no swirl jet. This means that the local heat transfer (Nu_{st}) is affected by the spacing between the jet and the plate as well as the jet swirling angle. This indicates that the increased swirl angle with increased plate-to-jet distance can significantly reduce the stagnation points' Nusselt number (Nu_{st}) and, consequently, the heat transfer rate. In addition to that at the small plate-to-jet distance, increasing the swirl angle increased the stagnation points' Nusselt number (Nu_{st}).

Figure 5 represents the swirl effect on the radial Nusselt number distribution at Z/D = 2. The Nu_{st} for all swirl numbers is higher than

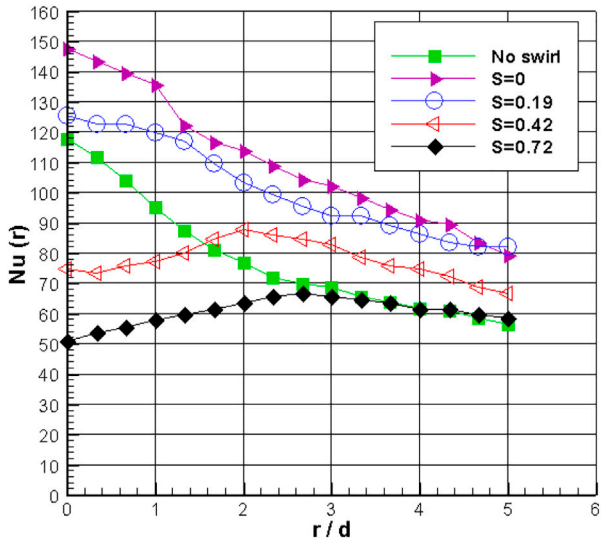

FIGURE 7
Local Nusselt number distribution with r/d at different swirl numbers for Z/D = 10.

a conventional jet (without a swirl generator). This increase is due to the interactions between the multiple jets in each swirl jet, which have an exit velocity greater than that of a conventional jet. This increase in the exit velocity is due to the reduction of the nozzle exit cross-sectional area for the same airflow rate. From this figure, it is also evident that, for Z/D = 2, the point of the maximum Nusselt number (Nu_{max} shifted from the stagnation point to a radial position r/D = 0.66, 0.66, 1, and 1.33 for S = 0, 0.19, 0.42, and 0.72, respectively. This shift of the peak local Nusselt number may have two reasons. The first is that the swirl generator causes the nozzle to act as a multi-channel jet, which causes stagnation points to not lie at the geometric center of the target plate because of the blockage area at the center of the swirl generator. The second reason is the spreading rate that increased with increasing the swirl number S. The first reason appears in the case of the swirl generator having a swirl number equal to zero (S = 0), but the second appeared strongly with an increase in swirl number. The first and second reasons are presented as the spreading rate increases with an increasing swirl number.

Figure 6 represents the swirl effect on the radial Nusselt number distribution at Z/D = 6. This figure shows that increasing the separation distance between the jet and the target plate to (Z/D = 6) reduces the local Nusselt number values compared with (Z/D = 2) values. It appears that the maximum Nusselt number for S = 0 and 0.19 is at the geometric center of the plate (conventional stagnation point), just like the one with no swirl. This is due to the spreading of the multiple jets losing their effect at a high Z/D distance, making the interaction between their sub-jet wall regions lie at the geometric center of the plate. However, for S = 0.42 and 0.72, the spreading rate is high in the lateral direction, causing the point of maximum Nusselt number (Nu_{max}) to shift far from the geometric center of the plate.

Figure 7 also represents the swirl effect on the radial Nusselt number distribution at Z/D = 10. It shows that increasing the separation distance between the plate and the air jet to Z/D = 10 reduces the local Nusselt number values compared with Z/D = 6, but the points of maximum Nusselt number lie at the geometric center of the plate for S = 0 and 0.19. S = 0.42 and 0.72 shifted to the right at r/d 2 and 2.7, respectively, with increased uniformity in heat transfer distribution.

The pressure drop of the nozzles was measured as 0.16, 0.19, 0.41, 0.81, and 1.83 for no swirl, S = 0.19, 0.42, and 0.72 respectively. The flow area ratios between the flow cross-sectional area to the no-swirl tube area were 1, 0.73, 0.62, 0.56, and 0.3 respectively. Thus, when using a constant inlet flow rate, decreasing the flow area ratio increased jet velocity, which increased the impingement on the plate.

5 Conclusion

In this study, an experimental test rig investigated the performance of the heat transfer of impingement jet cooling on a flat plate with and without swirling nozzles. The heat transfer measurements were performed with and without swirling air jets at different plate-to-jet distances to investigate the effect of swirling jets on heat transfer distributions near the stagnation point region at different Z/D distances. From this investigation, it can be concluded that swirl angle enhances heat transfer by producing multiple jets around the central hole with the high tangential velocity of the swirling jet. In addition:

1- For all cases used in this paper, the heat transfer distribution decreases with increased nozzle-to-plate distance.
2- Increasing the swirl number S increases heat transfer uniformity but decreases global heat transfer.
3- At the low plate-to-jet distance Z/D = 2, the point of maximum heat transfer is shifted to a radial position, depending on the swirl number. Stagnation-point heat transfer is enhanced by using a swirl air jet for swirl numbers 0, 0.19, 0.42, and 0.72 at Z/D = 2.
4- For both Z/D = 6 and 10, the stagnation point and stagnation region heat-transfer enhances only for swirl numbers 0 and 0.19.

Data availability statement

The original contributions presented in the study are included in the article/Supplementary Material; further inquiries can be directed to the corresponding author.

Author contributions

All authors listed have made a substantial, direct, and intellectual contribution to the work and approved it for publication.

Conflict of interest

The authors declare that the research was conducted in the absence of any commercial or financial relationships that could be construed as a potential conflict of interest.

Publisher's note

References

Ahmed-Zahir, U., Al-Abdeli, Y M., and Guzzomi, F G. (2016). Heat transfer characteristics of swirling and non-swirling impinging turbulent jets. *Int. J. Heat Mass Transf.* 102, 991–1003. doi:10.1016/j.ijheatmasstransfer.2016.06.037

Ahmed, Z. U., Al-Abdeli, Y. M., and Guzzomi, F. G. (2017). Flow field and thermal behaviour in swirling and non-swirling turbulent impinging jets. *Int. J. Therm. Sci.* 114, 241–256. doi:10.1016/j.ijthermalsci.2016.12.013

Ahmed, Z. U., Al-Abdeli, Y. M., and Guzzomi, F. G. (2016). Heat transfer characteristics of swirling and non-swirling impinging turbulent jets. *Int. J. Heat. Mass Transf.* 102, 991–1003. doi:10.1016/j.ijheatmasstransfer.2016.06.037

Alekseenko, S.V., Bilsky, A. V., Dulin, V. M., and Markovich, D. M. (2007). Experimental study of an impinging jet with different swirl rates. *Int. J. Heat Fluid Flow* 28, 1340–1359. doi:10.1016/j.ijheatfluidflow.2007.05.011

Baydar, E. (1999). Confined impinging air jet at low Reynolds numbers. *Exp. Therm. Fluid Sci.* 19, 27–33. doi:10.1016/s0894-1777(98)10044-4

Cardone, A. I. G., and Carlomagno, G. M. (2010). "IR wall heat transfer in swirling impinging jets," in *10th international conference on quantitative InfraRed thermography*, 27–30.

Colucci, D. W., and Viskanta, R. (1996). Effect of nozzle geometry on local convective heat transfer to a confined impinging air jet. *Exp. Therm. Fluid Sci.* 13, 71–80. doi:10.1016/0894-1777(96)00015-5

Debnath, S., Khan, M. H. U., and Ahmed, Z. U. (2020). Turbulent swirling impinging jet arrays: A numerical study on fluid flow and heat transfer. *Therm. Sci. Eng. Prog.* 19, 100580. doi:10.1016/j.tsep.2020.100580

Duda, J. C., Lagor, F. D., and Fleischer, A. S. (2008). A flow visualization study of the development of vortex structures in a round jet impinging on a flat plate and a cylindrical pedestal. *Exp. Therm. Fluid Sci.* 32, 1754–1758. doi:10.1016/j.expthermflusci.2008.05.001

Garimella, B., and Nenaydykh, B. (1996). Nozzle-geometry effects in liquid jet impingement heat transfer. *Int. J. Heat. Mass Transf.* 39, 2915–2923. doi:10.1016/0017-9310(95)00382-7

Gauntner, J. W., Livingwood, J. N. B., and Hrycak, P. (1970). *Survey of literature on flow characteristics of a single turbulent jet impinging on a flat plate*. NASA TN D-5652.

Greco, C. S., Paolillo, G., Ianiro, A., Cardone, G., and de Luca, L. (2018). Effects of the stroke length and nozzle-to-plate distance on synthetic jet impingement heat transfer. *Int. J. Heat Mass Transf.* 117, 1019–1031. doi:10.1016/j.ijheatmasstransfer.2017.09.118

Hattori, H., and Nagano, Y. (2004). Direct numerical simulation of turbulent heat transfer in plane impinging jet. *Int. J. Heat Fluid Flow* 25, 749–758. doi:10.1016/j.ijheatfluidflow.2004.05.004

Huang, L., and El-Genk, M. S. (1997). Heat transfer and flow visualization experiments of swirling, multi-channel, and conventional impinging jets. *Int. J. Heat Mass Transf.* 41, 583–600. doi:10.1016/s0017-9310(97)00123-3

Ikhlaq, M., Al-Abdeli, Y. M., and Khiadani, M. (2019). Transient heat transfer characteristics of swirling and non-swirling turbulent impinging jets. *Exp. Therm. Fluid Sci.* 109, 109917. doi:10.1016/j.expthermflusci.2019.109917

Lee, D. H., Won, S. J., Kim, Y. T., and Chung, Y. S. (2002). Turbulent Heat Transfer from a flat surface to a swirling round impinging jet. *Int. J. Heat. Mass Transf.* 45, 223–227. doi:10.1016/s0017-9310(01)00135-1

Markal, B. (2018). Experimental investigation of heat transfer characteristics and wall pressure distribution of swirling coaxial confined impinging air jets. *Int. J. Heat Mass Transf.* 124, 517–532. doi:10.1016/j.ijheatmasstransfer.2018.03.101

Martin, H. (1977). Heat and mass transfer between impinging gas jets and solid surfaces. *Adv. Heat Transf.* 13, 1–60.

Nuntadusit, C., Wae-hayee, M., Bunyajitradulya, A., and Eiamsa-ard, S. (2012). Visualization of flow and heat transfer characteristics for swirling impinging jet. *Int. Commun. Heat. Mass Transf.* 39, 640–648. doi:10.1016/j.icheatmasstransfer.2012.03.002

Owsenek, B. L., Cziesla, T., Mitra, N. K., and Biswas, G. (1997). Numerical investigation of heat transfer in impinging axial and radial jets with superimposed swirl. *Int. J. Heat. Mass Transf.* 40, 141–147. doi:10.1016/s0017-9310(96)00086-5

Öztekin, E., Aydin, O., and Avcı, M. (2013). Heat transfer in a turbulent slot jet flow impinging on concave surfaces. *Int. Commun. Heat. Mass Transf.* 44, 77–82. doi:10.1016/j.icheatmasstransfer.2013.03.006

Oztekin, E., Aydin, O., and Avci, M. (2012). Hydrodynamics of a turbulent slot jet flow impinging on a concave surface. *Int. Commun. Heat. Mass Transf.* 39, 1631–1638. doi:10.1016/j.icheatmasstransfer.2012.10.015

Paolillo, G., Greco, C. S., Astarita, T., and Cardone, G. (2022). Effects of the swirl number, Reynolds number and nozzle-to-plate distance on impingement heat transfer from swirling jets. *Int. J. Heat Mass Transf.* 197, 123284. doi:10.1016/j.ijheatmasstransfer.2022.123284

Singh, P., Aider, Y., and Kaur, I. (2023). Swirl jet impingement heat transfer: Effect of jet-to-target spacing, jet Reynolds number and orientation with flat target. *Int. J. Therm. Sci.* 184, 107993. doi:10.1016/j.ijthermalsci.2022.107993

Tesar, V. (2009). Enhancing impinging jet heat or mass transfer by fluidically generated flow pulsationfluidically generated flow pulsation. *Chem. Eng. Res. Des.* 87, 181–192. doi:10.1016/j.cherd.2008.08.003

Ward, J., and Mahmood, M. (1982). "Heat transfer from a turbulent, swirling, impinging jet," in *Proceedings of the 7th international heat transfer Conference HTD-3*, 401–407.

Wen, M. Y., and Jang, K. J. (2003). An impingement cooling on a flat surface by using circular jet with longitudinal swirling strips. *Int. J. Heat Mass Transf.* 46, 4657–4667. doi:10.1016/s0017-9310(03)00302-8

Xu, L., Yang, T., Sun, Y., Xi, L., Gao, J., Li, Y., and Li, J. (2021). Flow and heat transfer characteristics of a swirling impinging jet issuing from a threaded nozzle. *Case Stud. Therm. Eng.* 25, 100970. doi:10.1016/j.csite.2021.100970

Yang, G., Chio, M., and Lee, J. S. (1999). An experimental study of slot jet impingement cooling on concave surface: Effects of nozzle configuration and curvature. *Int. J. Heat. Mass Transf.* 42, 2199–2209. doi:10.1016/s0017-9310(98)00337-8

Yang, T., Sun, Y., Xu, L., Xi, L., Gao, J., and Li, Y. (2023). Comparative study on flow and heat transfer characteristics of swirling impingement jet issuing from different nozzles. *J. Therm. Sci.* 184, 107914. doi:10.1016/j.ijthermalsci.2022.107914